AMERICAN SOCIETY FOR MICROBIOLOGY | Microbiology Spectrum

RESEARCH ARTICLE

A Critical Role for p53 during the HPV16 Life Cycle

Christian T. Fontan,[a] Claire D. James,[a] Apurva T. Prabhakar,[a] Molly L. Bristol,[a,d] Raymonde Otoa,[a] Xu Wang,[a] Elmira Karimi,[a] Pavithra Rajagopalan,[b] Devraj Basu,[b,c] Iain M. Morgan[a,d]

[a]Philips Institute for Oral Health Research, School of Dentistry, Virginia Commonwealth University (VCU), Richmond, Virginia, USA
[b]Department of Otorhinolaryngology, University of Pennsylvania, Philadelphia, Pennsylvania, USA
[c]The Wistar Institute Cancer Center, Philadelphia, Pennsylvania, USA
[d]VCU Massey Cancer Center, Richmond, Virginia, USA

ABSTRACT Human papillomaviruses (HPV) are causative agents in ano-genital and oral cancers; HPV16 is the most prevalent type detected in human cancers. The HPV16 E6 protein targets p53 for proteasomal degradation to facilitate proliferation of the HPV16 infected cell. However, in HPV16 immortalized cells E6 is predominantly spliced (E6*) and unable to degrade p53. Here, we demonstrate that human foreskin keratinocytes immortalized by HPV16 (HFK+HPV16), and HPV16 positive oropharyngeal cancers, retain significant expression of p53. In addition, p53 levels increase in HPV16+ head and neck cancer cell lines following treatment with cisplatin. Introduction of full-length E6 into HFK+HPV16 resulted in attenuation of cellular growth (in hTERT immortalized HFK, E6 expression promoted enhanced proliferation). An understudied interaction is that between E2 and p53 and we investigated whether this was important for the viral life cycle. We generated mutant genomes with E2 unable to interact with p53 resulting in profound phenotypes in primary HFK. The mutant induced hyper-proliferation, but an ultimate arrest of cell growth; β-galactosidase staining demonstrated increased senescence, and COMET assays showed increased DNA damage compared with HFK+HPV16 wild-type cells. There was failure of the viral life cycle in organotypic rafts with the mutant HFK resulting in premature differentiation and reduced proliferation. The results demonstrate that p53 expression is critical during the HPV16 life cycle, and that this may be due to a functional interaction between E2 and p53. Disruption of this interaction has antiviral potential.

IMPORTANCE Human papillomaviruses are causative agents in around 5% of all cancers. There are currently no antivirals available to combat these infections and cancers, therefore it remains a priority to enhance our understanding of the HPV life cycle. Here, we demonstrate that an interaction between the viral replication/transcription/segregation factor E2 and the tumor suppressor p53 is critical for the HPV16 life cycle. HPV16 immortalized cells retain significant expression of p53, and the critical role for the E2-p53 interaction demonstrates why this is the case. If the E2-p53 interaction is disrupted then HPV16 immortalized cells fail to proliferate, have enhanced DNA damage and senescence, and there is premature differentiation during the viral life cycle. Results suggest that targeting the E2-p53 interaction would have therapeutic benefits, potentially attenuating the spread of HPV16.

KEYWORDS human papillomavirus, E2, p53, cervical cancer, head and neck cancer, life cycle, comet assay, senescence, interaction, comet, dna binding, dna damage, papillomavirus

HPV16 infection causes half of cervical cancers and up to 90% of HPV-positive oropharyngeal cancers (1). Despite advances in vaccination, the prevalence in HPV-associated oropharyngeal cancer continues to rise, contributing to an ongoing public health crisis without any effective antiviral therapies (2–5).

Editor Samuel K. Campos, University of Arizona

Address correspondence to Iain M. Morgan, immorgan@vcu.edu.

The authors declare no conflict of interest.

Received 9 March 2022
Accepted 22 April 2022
Published 24 May 2022

HPV infects basal epithelial cells and delivers its circular 8kbp DNA genome into the nucleus of the host. Consequently, cellular host factors initiate transcription from the viral long control region (LCR) (6). The viral mRNA is expressed from a single transcript which is then processed, spliced and translated into individual viral proteins. In high-risk HPV infection, the viral oncoproteins E6 and E7 contribute to cellular transformation and cancer progression by targeting several cellular proteins, including tumor suppressors p53 and pRb, respectively (7–11).

HPV uses two proteins to initiate replication of the viral episome. The E2 protein homodimerizes via a carboxyl terminus domain and binds to four 12-bp palindromic sequences within the viral LCR and origin (12). Via its amino terminus, E2 recruits the viral helicase E1 to the origin which forms a di-hexamer that replicates the viral genome with the assistance of host polymerases (13, 14). Upon initial infection, the HPV genome replicates to 20–50 copies and maintains this copy number as the infected cell migrates through the epithelium. As the infected cell differentiates and reaches the upper layers, the viral genome amplifies and expresses the L1 and L2 capsid proteins that promote virus assembly and shedding (15–17).

E2 has additional roles in the viral life cycle. E2 can promote or repress viral transcription depending on protein concentration (18). E2 binds to host mitotic chromatin to facilitate viral segregation, resulting in sorting of viral episomes into daughter nuclei following mitosis (19). E2 also regulates expression of host genes important in the viral life cycle and cancer progression (20–24).

The tumor suppressor p53 primarily functions as a transcription regulatory factor during cellular stress and DNA-damage, leading to cell cycle arrest, senescence, and apoptosis (25–30). In HPV infection, the 150 amino acid E6 oncoprotein interferes with the transcriptional activity of tumor suppressor p53, as well as induces its degradation (7, 9, 31). Direct degradation is initiated by the formation of a complex with p53 and the host partner protein E6AP, which is a ubiquitin ligase. E6 directs the ligase activity of E6AP to p53, promoting its degradation via the proteasome (7, 31–33). This is in direct contrast with many HPV-negative cancers where p53 often becomes mutationally inactivated (34, 35). The degradation of p53 by HPV is also regulated by alternative splicing of high-risk E6 proteins, resulting in a short modulatory isoforms of the oncoprotein such as E6* and E6*I which do not bind to p53 and can inhibit E6-E6AP-p53 complex formation preventing p53 degradation in a cell cycle specific manner (36–38). We, and others, have reported that expression of alternatively spliced forms of E6 are more dominant compared to full-length E6 in HPV-positive head and neck cancer, and ectopic expression of these isoforms have anti-tumorigenic effects (38–41). The disruption of the E6-E6AP-p53 degradation complex by E6* and E6*I, allowing for p53 expression, suggests that p53 expression may be important in HPV immortalized cells.

Another reported viral interactor with p53 is E2. E2 proteins from high-risk HPVs can bind to p53 and this interaction can trigger apoptosis in cervical cancer cells (42, 43). Additionally, E2 replication function is regulated by this interaction with p53 as overexpression of p53 reduces viral replication (44). This led us to hypothesize that in HPV16 immortalized cells, residual p53 is necessary to maintain a healthy viral life cycle, perhaps via an interaction with E2.

Here, we demonstrate that p53 expression is clearly detectable in a variety of cell lines and tumors immortalized by HPV16 (45, 46). Depletion of residual p53 by overexpression of full-length E6 protein led to a significant reduction in cellular proliferation in keratinocytes immortalized by wild-type HPV16. Expression of a mutant E6 protein lacking p53 binding had no effect on cell growth. To determine whether an interaction between E2 and p53 was important for cellular proliferation of HPV16 positive cells, we generated an HPV16 genome with point mutations in the E2 gene compromising p53 binding HPV16(-p53) (42, 43). Both wild type and p53 mutant binding E2 proteins have identical DNA binding activity *in vivo*. Keratinocytes were then immortalized by this mutant. Remarkably, compared to wild type HPV16, HPV16(-p53) mutant cells, following an initial burst in proliferation, stopped growing and had increased levels of

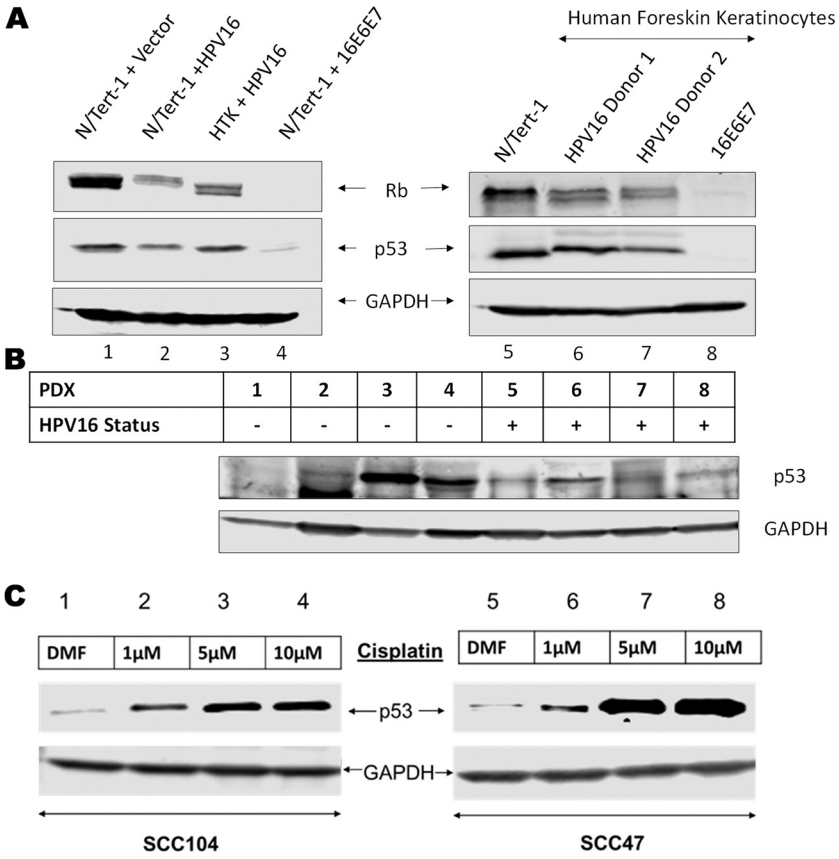

FIG 1 Tumor suppressor p53 expression is conserved in HPV16 immortalized cell lines and patient derived xenografts. (A) Western blot analysis of p53 and pRb in N/tert-1 cells stably expressing the HPV16 genome (lane 2), HPV16 E6+E7 (lane 4) or empty vector (lane 1) compared to Human tonsillar keratinocytes immortalized with HPV16 (lane 3). Two independent human foreskin keratinocyte (HFK) donors were immortalized with wild-type HPV16 (lanes 6 and 7) or exogenous expression of the HPV16 E6 and E7 oncogenes (lane 8, cells from donor 1). (B) Western blot analysis of p53 expression in 4 HPV-negative and 4 HPV-positive patient derived xenografts. (C) p53 expression following 24-h cisplatin treatment of primary HPV-positive head and neck cancer cell lines (SCC47 and SCC104) DMF solvent only was used as drug-free control. All Western blots utilized GAPDH as an internal loading control.

senescence, and accumulated DNA breaks as evidence by single-cell gel electrophoresis assay (COMET). When subjected to differentiation via organotypic raft culturing, these mutant cells had reduced proliferation leading to marked reduction in raft thickness. There was also a reduction in viral replication markers in the mutant cells. These results suggest that although p53 is downregulated by E6 in high-risk HPV infection, p53 is necessary to permit HPV induced proliferation and that the interaction with E2 plays an important role in the requirement for p53 expression.

RESULTS

Tumor suppressor p53 is expressed in HPV16 immortalized cells and is critical for their optimal growth. Previous studies demonstrated that alternative splice variants (E6*) are the dominant E6 transcripts in HPV associated head and neck cancer, preventing E6-E6AP-p53 complex formation and inhibiting p53 degradation (36–41). We confirmed the presence of p53 in a series of HPV16 positive cell lines (Fig. 1). Expression of the entire HPV16 full genome in N/Tert-1 cells results in partial reduction in p53 compared to near complete abrogation by expression of HPV16 E6 and E7 (Fig. 1A compare lanes 2 and 4 to lane 1). Moreover, human tonsil cells immortalized by HPV16 retain p53 expression similar to N/Tert-1 cells (compare lane 1 to 3). To investigate these findings further, we studied two independent donors of human foreskin keratinocytes (HFK) immortalized with HPV16, each grown as pools. In both donor

lines, p53 levels were less reduced compared to HFK immortalized by HPV16 E6 and E7 overexpression (lanes 5–8). It is noticeable that the p53 in the HPV16 immortalized HFK (lanes 6 and 7) have reduced mobility suggesting differential posttranslational modification of p53 compared with N/Tert-1 cells. Such modifications are known to alter p53 function, therefore although p53 is expressed in these cells modifications may be altering its function (47). To determine whether this expression is affected by tumor microenvironment, we surveyed p53 expression in 8 patient derived xenografts (PDX) from oropharyngeal and oral cavity carcinomas (four HPV16 positive and four negative) (45, 46). All HPV16 positive PDX samples and 3 out of 4 HPV negative retained detectable p53 expression illustrating no clear association between HPV status and p53 expression (Fig. 1B). HPV-negative PDXs 1–3 have mutant p53 while PDX 4 is wild type for p53. All HPV positive PDXs retained wild-type p53. Platinum based DNA-damaging agents such as cisplatin are critical in the treatment of late-stage systemic head and neck cancers (48–51). Because DNA-damage is known to stabilize and activate p53, and p53 is most often wild-type in HPV-positive cancers, we predicted that in HPV+ head and neck cancer cell lines the expression of active wild-type p53 can be promoted by cisplatin treatment. We confirmed dose-dependent cisplatin induced p53 expression in SCC-47 and SCC-104 cells (Fig. 1C). These results demonstrate that p53 expression is retained in many cell lines immortalized by the HPV16 genome and can be induced following DNA-damage. This suggests that although E6 degrades p53 to help promote cell immortalization and carcinogenesis, HPV16 retains p53 expression, indicating that p53 may play an important role in the HPV16 life cycle.

To determine whether reduction of p53 compromises the growth of HPV16 immortalized cells we introduced full-length E6 (using a retroviral delivery of the E6 gene which does not allow alternative splicing) into N/Tert-1 (foreskin keratinocytes immortalized by telomerase) and HFK+HPV16 cells. Fig. 2A demonstrates that the additional expression of E6 in N/Tert-1 cells result in significantly increased cellular proliferation as has been described (52). However, introduction of E6 into HFK+HPV16 resulted in an attenuation of cell growth (Fig. 2B). Because E6 possesses several mechanisms for regulating cellular proliferation independent from p53 degradation, we attempted to isolate these other mechanisms by expressing an E6 mutant unable to promote degradation of p53 but retaining all other known functions. The "8S9A10T" mutant (designated E6Δp53 in this study for clarity) is deficient in p53 binding but can still immortalize cells and activate telomerase as efficiently as E6 wild type (53). In this mutant, residues Arg 8, Pro 9 and Arg 10 are replaced with Ser, Ala and Thr, respectively. This mutant did not have a deleterious effect on cell growth indicating that it is E6 targeting of p53 attenuates cellular proliferation. Additionally, we found that these proliferation rates inversely correlated with senescence levels (Fig. 2C and D). In the HFK+HPV16+E6 cells, we noticed that over time the cells began proliferating once again. To determine whether the recovered cells had a restoration of p53 protein levels we carried out Western blots of HFK+HPV16+E6 cells at different stages following E6 introduction (Fig. 2E). Lane 4 demonstrates that there is an initial reduction in p53 protein levels in these cells immediately following selection compared with control cells (compare lane 4 with lane 3). However, following 13 days of culturing (when we noticed proliferation begin to restore to that of the control cells) there is a restoration of p53 protein expression (compare lane 7 with lane 4). These results suggest that reduction of p53 protein may lead to growth attenuation and enhanced senescence of HFK+HPV16 cells. They also suggest that to begin to proliferate again, restoration of p53 likely helps promote growth in the HFK+HPV16+E6 cells. We monitored the exogenous E6 RNA levels (Fig. 2F). There is a clear reduction in the E6 RNA expressed from the exogenous vector between days 0 and 13 correlating with the restoration of p53 protein expression and cellular proliferation. When we analyzed for E6 protein expression via Western blot, while we did not notice an appreciable change in E6 protein levels, we found that there was a significant increase of E6Δp53 expression compared to wild-type E6 at both time points (Fig. 2G). This supports our

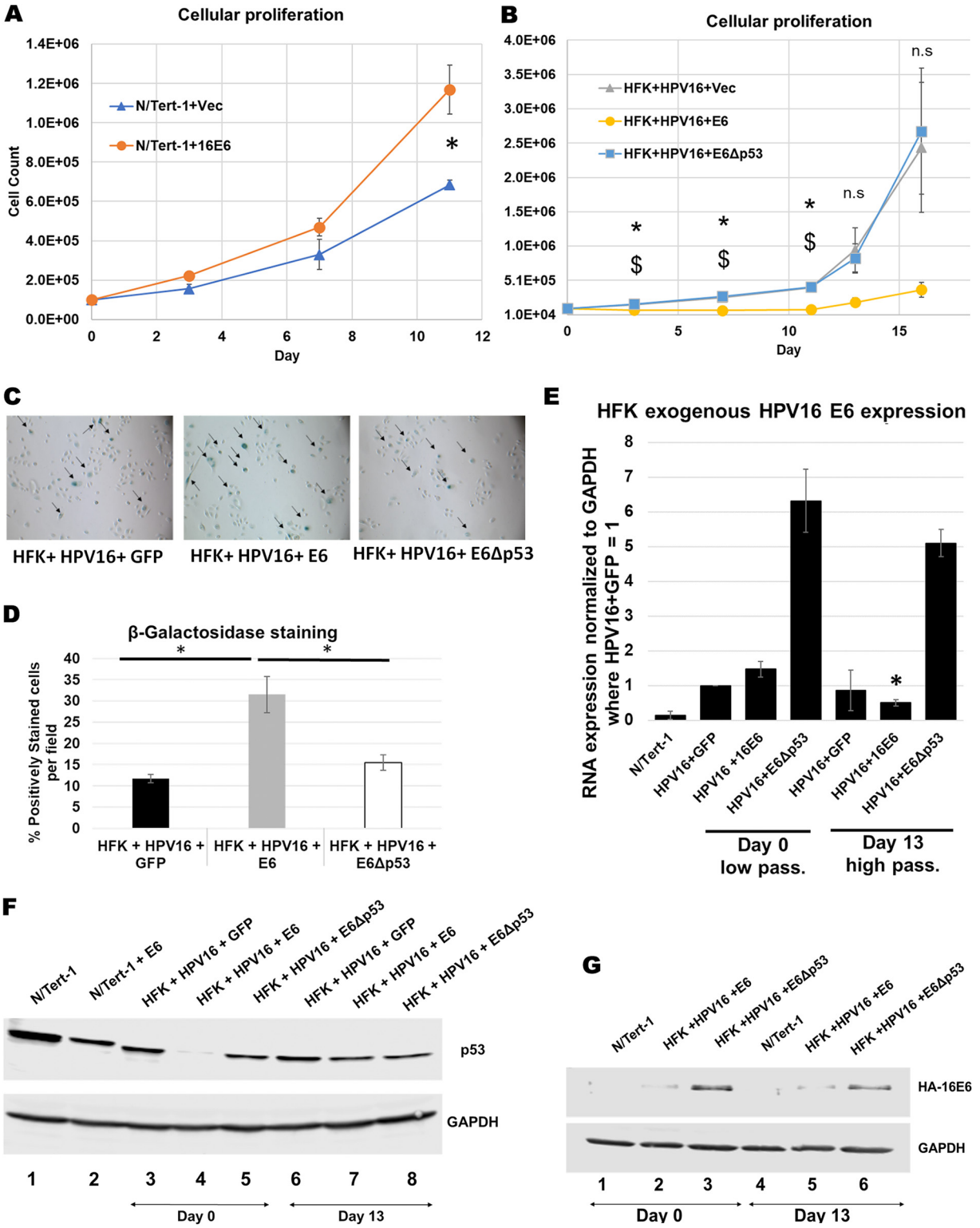

FIG 2 p53 reduction in via introduction of full-length HPV16 E6 reduces cellular proliferation in HPV16 immortalized foreskin keratinocytes. (A) 11-day growth curve of N/Tert-1 cells expressing exogenous HPV16 E6 compared to empty vector. (B) 13-day growth curve of human foreskin keratinocytes immortalized by HPV16 and stably expressing exogenous full-length E6, mutant E6 that does not bind and degrade p53 (E6Δp53) or GFP control vector. (C) Senescence staining of cells in B at day 11. Arrows indicate positively staining cells. (D) Quantification of senescence staining in C as percent positively stained per field. Western blot analysis of p53 expression following transfection of E6 plasmids (day 0) and after growth rate recovery of HFK+HPV16+E6 (day 13). (E) Western blot analysis of p53 in HFKs with exogenous E6 and E6Δp53 expression at day 0 and day 13. GAPDH was used as internal loading control. (F) RT-qPCR analysis of exogenous GFP, E6 and E6Δp53 expression at day 0 and day 13 using primers against FLAG-HA tag. Relative quantity calculated by the $\Delta\Delta C_T$ method using GAPDH as an internal control. Bonferroni correction utilized when applicable. (G) Western blotting of the indicated extracts using FLAG antibody (the E6 is double tagged with HA and FLAG).

claim that expression of E6 is more deleterious to growth than E6Δp53 in HFK+HPV16 and this is likely due to p53 degradation.

Overall, these results demonstrate that p53 is expressed in HPV16 immortalized cells, and that this expression may be critical for continuing proliferation of these cells. We next moved on to investigate possible reasons for the requirement of p53 expression in HFK+HPV16 cells.

Disruption of p53 interaction with the HPV16 E2 protein attenuates cell growth and blocks the viral life cycle. A known and relatively understudied interaction of p53 with HPV16 is the direct physical interaction with E2 (43). We generated an E2 mutant predicted not to interact with p53 by performing site directed mutagenesis. Residues aspartate 388, tryptophan 341, and aspartate 344 were all mutated to alanine within the E2 plasmid, resulting in inability for E2 to interact with p53 (E2[-p53]). We generated stable N/Tert-1 cell lines expressing this mutant, as we have done for wild-type E2 (E2-WT) (43). There was robust, stable expression of E2-WT and E2(-p53) in N/Tert-1 cells (Fig. 3A, lane 3). Immunoprecipitation with a p53 antibody brought down p53, and E2-WT co-immunoprecipitated with p53 while E2(-p53) did not (Fig. 3B, compare lanes 2 and 3). To demonstrate that E2(-p53) was functional we carried out transcriptional studies in N/Tert-1 cells. Because the binding of p53 takes place in the DNA-binding domain (DBD) of E2, we confirmed that the mutant E2 retained DNA-binding function. Both E2-WT and E2(-p53) were able to repress transcription from the HPV16 long control region (LCR) efficiently and comparatively (Fig. 3C). We also measured that transcriptional activation function of E2-WT and E2(-p53) (Fig. 3D). While E2(-p53) is able to activate transcription, it was significantly compromised in this function compared with E2-WT (compare lanes 5–7 with lanes 2–4). We conclude from these results experiments that E2(-p53) is nuclear and able to bind to its DNA target sequences but that its transcriptional activation property (but not repression) is attenuated.

We further explored the DNA binding and p53 interaction properties of the E2 (-p53) mutant. The experiment in Fig. 3A and B was repeated and the pull-down of the E2 proteins by p53 quantitated (normalized to the input protein levels). The interaction between E2 and p53 was significantly reduced with the E2(-p53) mutant compared with E2-WT (Fig. 4A). Given that the E2(-p53) protein was a poorer transactivator than E2-WT (Fig. 3D) we wanted to confirm that this was not due to a reduction in DNA binding properties. To do this we transfected either the pHPV16LCR-luc (the luciferase plasmid used in the repression assays in Fig. 3C) or ptk6E2-luc (the plasmid used in the transcriptional activation assays in Fig. 3D) into N/Tert-1+Vec, N/Tert-1+E2-WT or N/Tert-1+E2(-p53). Three days following transfection chromatin was prepared from the transfected cells and E2 chromatin immunoprecipitation (ChIP) assays carried out, as we have described previously (54, 55). Fig. 4B and C demonstrate that both E2-WT and E2(-p53) have no difference in their ability to bind to either pHPV16LCR-luc or ptk6E2-luc, respectively. Recently we demonstrated that E2-WT can bind to and repress transcription from the TWIST1 promoter (20). Both E2-WT and E2(-p53) bound equivalently to this endogenous promoter in N/Tert-1 cells (Fig. 4D). Next, we investigated the DNA replication properties of E2(-p53). Ordinarily we perform these assays in C33a cells but these have a mutant p53 protein. Therefore, we used U2OS cells (that have wild type p53) that we have demonstrated supports E1-E2 mediated DNA replication (56). Fig. 3E demonstrates that the E2(-p53) mutant has a compromised interaction with p53 in U2OS cells compared with E2-WT and Fig. 3F illustrates that E2(-p53) and E2-WT have similar DNA replication properties. Moreover, we confirmed that this mutant does not have a disrupted affinity to the E1 helicase. Overall, these results demonstrate that the DNA binding properties of E2(-p53) are not compromised.

Having confirmed that the E2(-p53) mutant was functional, we introduced identical mutations that abrogate E2-p53 interaction into the entire HPV16 genome (HPV16 [-p53]). We introduced the wild type and mutant HPV16 genomes into 2 independent primary human foreskin cell populations and grew each donor as pools. We recently used these methods to investigate the role of the E2-TopBP1 interaction in the viral life cycle (57). Both the wild type and mutant genomes efficiently immortalized both HFK

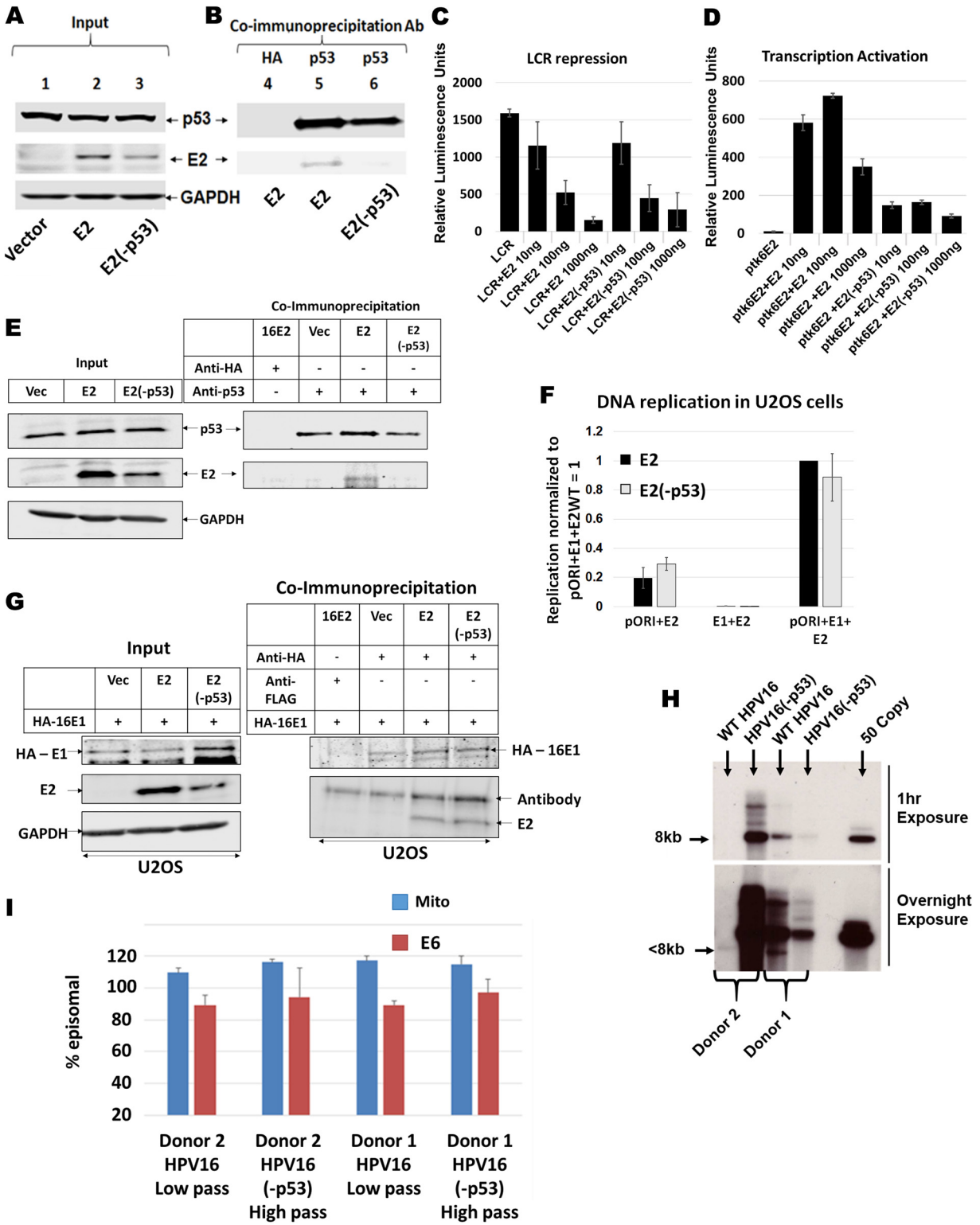

FIG 3 Generation and characterization of p53 binding mutant of HPV16 E2 (E2-p53) in N/Tert-1 cells. (A) Input Western blot of stably expressing E2 and E2(-p53) in N/Tert-1 Cells. For E2(-p53), residues W341, D344 and D338 were mutated to alanine as previously described (42, 43). (B) Co-immunoprecipitation pull down of E2 using polyclonal antibody against p53. (C) HPV16 long control region repression assay of wild-type E2 and E2(-p53). N/Tert-1 cells were transiently transfected with 1 μg pHPV16-LCR-Luciferase reporter plasmid along with 10 ng, 100 ng, or 1000 ng of E2 or E2(-p53) plasmid. (D) E2 transcriptional activity assay of wild-type E2 and E2(-p53). Similar to LCR repression assay, N/Tert-1 cells were transiently transfected with 1 μg pTK6E2-Luciferase reporter plasmid along with increasing amounts of E2 wild-type and E2(-p53) plasmids. For (C) and (D), relative luminescence units were calculated by normalizing absolute luminescence readouts to input protein concentration. (E) U2OS cells stably expressing E2-WT and E2(-p53) were generated and a p53 co-immunoprecipitation carried

(Continued on next page)

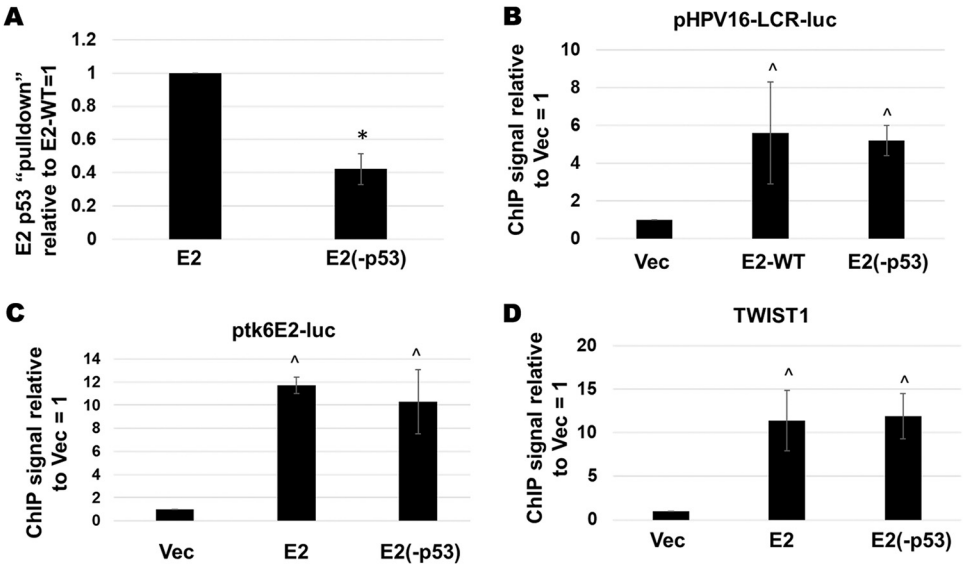

FIG 4 E2-WT and E2-p53 bind equally efficiently to DNA target sites *in vivo*. (A) The immunoblot and co-immunoprecipitation shown in Fig. 3A was repeated and quantitated relative to the E2 levels in the input blot. There was a significant reduction in the ability of E2(-p53) to interact with p53 compared with E2-WT as indicated by *, *P*-value < 0.05. (B) The indicated N/Tert-1 cell lines were transfected with 1 μg of pHPV16-LCR-luc. Three days following transfection chromatin was prepared and E2 chromatin immunoprecipitation carried out followed by detection of the luciferase gene present in pHPV16-LCR-luc. Results were standardized to input chromatin and then normalized to Vec = 1. There was a significant increase in signal in both E2-WT and E2(-p53) binding compared with Vec, but no significant difference between E2-WT and E2(-p53) (^, *P*-value < 0.05). (C) The indicated N/Tert-1 cell lines were transfected with 1 μg of ptk6E2-luc. Three days following transfection chromatin was prepared and E2 chromatin immunoprecipitation carried out followed by PCR detection of the luciferase gene present in pHPV16LCR-luc. Results were standardized to input chromatin and then normalized to Vec = 1. There was a significant increase in signal in both E2-WT and E2(-p53) binding compared with Vec, but no significant difference between E2-WT and E2(-p53) (^, *P*-value < 0.05). (D) E2-WT and E2(-p53) have similar DNA binding properties to the endogenous TWIST1 promoter, and both are significantly higher than the signal obtained in Vec control cells (^, *P*-value < 0.05).

donor cells. We carried out Southern blotting on *SphI* cut DNA (a single cutter for the HPV16 genome) (Fig. 3H). To further characterize the status of the genomes in these cells we used TV exonuclease assays (this assay is based on the fact that episomal HPV16 genomes are resistant to exonuclease digestion) (58, 59). This assay demonstrated that the viral DNA in the immortalized donor cell lines retained a predominantly episomal status, irrespective of whether the viral genomes were wild-type or HPV16(-p53) (Fig. 3I). It is noticeable in Fig. 3H that there is a wide range of viral genome copy number in the HFK immortalized cells. In Donor 1 there is a high level of HPV16-WT DNA with a reduced level of HPV16(-p53), although the overnight exposure demonstrates the robust presence of both viral genomes in the immortalized cells. In Donor 2 there was a much reduced level of HPV16-WT DNA compared with HPV16

FIG 3 Legend (Continued)
out. Left panel, input; right panel, co-IP. (F) Transient DNA replication assays were carried out on U2OS cells transfected with pOri, E1 or the indicated E2. Both E1+E2-WT and E1+E2(-p53) increased replication similarly, both significantly above background. (G) HA tagged E1 was transfected into the indicated cell lines and a HA co-immunoprecipitation carried out. Left panel, input; right panel, co-IP. (H) Southern blot of SphI digested DNA (cuts the HPV16 genome once) from the indicated immortalized human foreskin keratinocytes. An over exposure of this blot indicated a band in Donor 2 wild-type cells that migrated around 7.5kbp, indicating a part of the genome may have been lost during immortalization. PCR demonstrates that viral DNA is in these cells, and they are immortalized. With donor 1 there is less DNA with the mutant genome than the wild type, the opposite of Donor 2. Therefore, the mutation did not trend toward influencing the levels of DNA in the immortalized HFK. (I) TV exonuclease digestion assay to determine viral genome status. We looked at GAPDH in this assay and called the ΔCt for GAPDH 100% degradation, then we estimated the resistance of both mitochondrial (mito) DNA and HPV16 (E6) to degradation. In all cases the HPV16 DNA is predominantly episomal. As an example, if the ΔCt for GAPDH was 10 following exonuclease treatment, and the ΔCt for mito and E6 equals 1, then they were estimated as 90% episomal DNA (mitochondria have circular genomes that are resistant to the exonuclease). Low pass indicates low passage, 7 or less. High pass indicates high passage, 12 or greater. This demonstrates that, even following prolonged culture, there is no shift toward integration of the HPV16 genomes. The results shown are from duplicate or triplicate experiments, and standard error bars are shown.

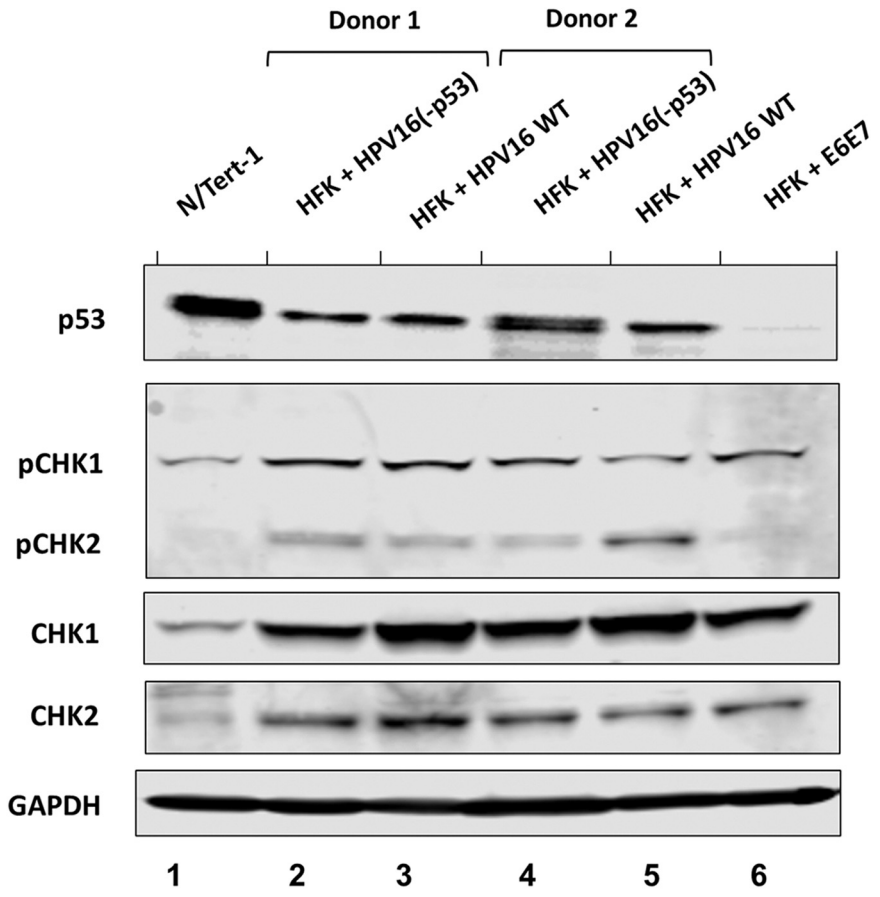

FIG 5 Generation and characterization of HPV16-p53 immortalized human foreskin keratinocytes (HFKs). p53 protein expression in two independent HFK donors immortalized by wild-type HPV16 (Lanes 3 and 5) and HPV16(-p53) (Lanes 2 and 4). N/Tert-1 and HFK immortalized by E6 and E7 are provided for reference (lanes 1 and 6, respectively). All lines were grown as pools. Activation of the ATR and ATM DNA-damage pathways in immortalized HFKs. ATR and ATM activation by HPV16 leads to phosphorylation of Checkpoint kinases 1 and 2, respectively, and serve as markers for HPV infection and replication.

(-p53), the opposite of Donor 1. In addition, there is a small deletion in the HPV16-WT DNA as demonstrated in the lower panel (it is less than 8kbp). However, all of the viral genomes are predominantly episomal in all of the lines as demonstrated in Fig. 3I. In the growth and life cycle studies described in Fig. 5, 6 and 7, the HPV16(-p53) genome containing cells both behave very similarly and very differently from the HPV16-WT cells, demonstrating that the differences observed are not due to the variation in copy number.

Next, we investigated the expression of markers relevant to HPV infection in HFKs. Fig. 5A demonstrates that p53 levels are similarly reduced in HFK+HPV16 and HFK+HPV16(-p53) cells compared with N/Tert-1 cells (compare lanes 2–5 with lane 1). For comparison, cells immortalized with an E6/E7 expression vector had almost no p53 expression (lane 6), likely due to the inability of the E6 to be spliced to E6* variants with this expression vector. To further characterize these cell lines, we investigated whether the DNA damage response is turned on as HPV infections activate both the ATR and ATM pathways. We investigated the phosphorylation status of CHK1 and CHK2 as surrogate markers for activation of these DNA damage response kinases (Fig. 5B). Compared with N/Tert-1 cells there is an overall increase of CHK1 and CHK2 levels in cells immortalized with HFK+HPV16, HFK+HPV16(-p53) or E6/E7 expression. CHK1 and CHK2 phosphorylation is also elevated in the presence of all of the HPV16 positive cells compared with N/Tert-1 cells. It is important to note that E6 and E7

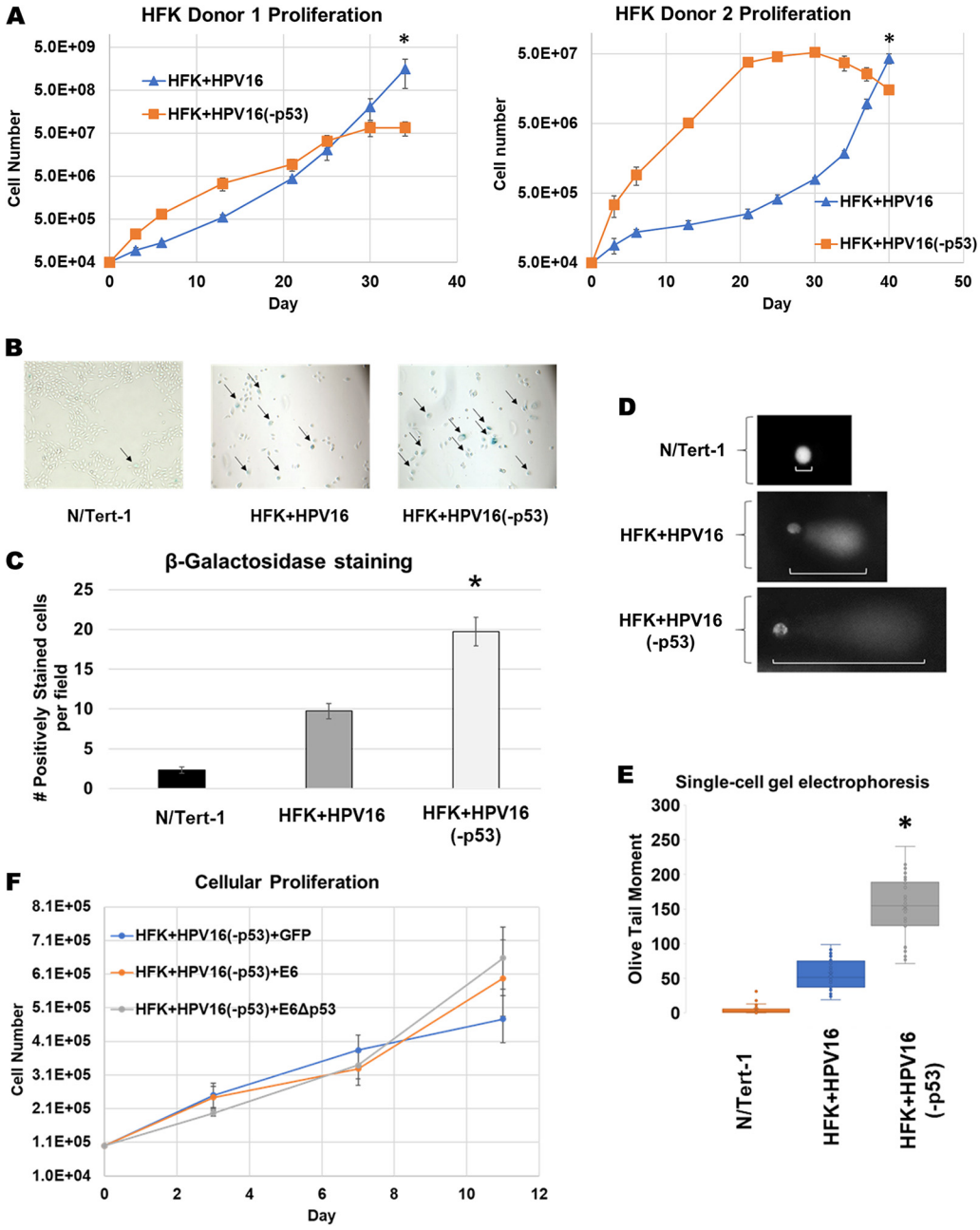

FIG 6 HFKs immortalized by HPV16-p53 exhibit aberrant growth phenotype, elevated levels of senescence and increased DNA damage and fragmentation. (A) Extended growth curve on HFK's immortalized by wild-type HPV16 and HPV16(-p53). Cells were grown over a period of 34–40 days depending on HFK donor cell line. In general, donor 1 proliferated quicker than donor 2 regardless of HPV genome status. (B) β-galactosidase staining as a marker of senescence for proliferating HFK+HPV16 and HFK+HPV16(-p53) cells compared to N/Tert-1 cells. Images taken at 10×. Five random fields were imaged per replicate per cell line. Representative image presented with positively stained cells marked by arrows. (C) Quantification of β-galactosidase staining. Average number of positively stained cells per high power field were calculated by a blinded observer +/- SEM. (D) Single-cell gel electrophoresis (COMET) Assay. Cells were grown in 24-well plate for 24 h then trypsinized, washed, resuspended in 0.5% low molecular weight agarose, and subjected to single cell gel electrophoresis. DNA was stained with DAPI. Five randomly selected fields were imaged at 20× per replicate per cell line. Representative comets are presented with white bars highlighting comet tails. (E) The olive-tail moments (OTMs) of all nonoverlapping comets in each high-power field were quantified using CaspLab COMET assay software. Average OTM +/- SEM. *$P < 0.05$ for HFK+HPV16 versus HFK+HPV16-p53. \$$P < 0.05$ for HFK+HPV16 versus N/Tert-1. Bonferoni correction used where applicable. (F) Eleven-day growth curve on HFK+HPV16(-p53) stably expressing exogenous E6, E6Δp53 or GFP control.

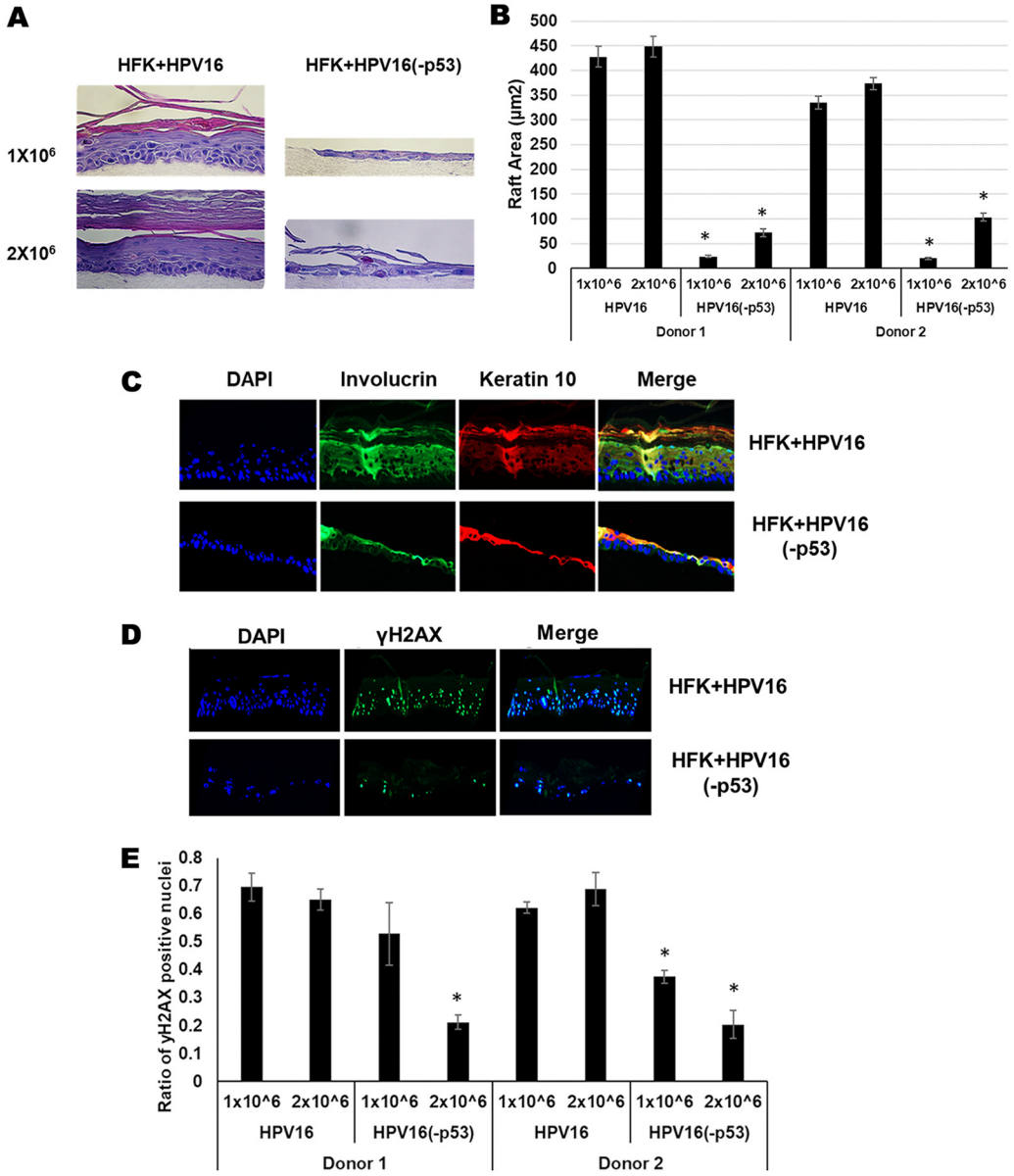

FIG 7 Organotypically rafted HFKs immortalized by HPV16-p53 exhibit aberrant life cycle with dysregulated differentiation, lower markers of viral replication and overall reduced raft proliferation. (A) Organotypic raft cultures and H&E staining of samples from Fig. 5. HFKs were seeded onto collagen matrices at densities of 1×10^6 (upper panels) and 2×10^6 (lower panels). (B) The experiment in A was repeated in a second independent HFK donor and average raft areas were calculated for each donor using a Keyence imaging system. (C) HFK rafts stained using indicated antibodies as markers of keratinocyte differentiation. (D) DNA damage and viral replication marker γ-H2AX was stained for in HPV16 and HPV16(-p53) HFK rafts. (E) γ-H2AX staining was repeated in a second HFK donor and quantified using a Keyence imaging system.

immortalization of HFK induced phosphorylation of CHK1 but not CHK2 compared with the entire genome (Lane 6). This is likely due to the ATM pathway being largely activated by viral replication rather than by the viral oncogenes E6 and E7 which we have previously reported (60). Overall, these results suggest that markers of HPV16 infection are activated in HFK cells immortalized with HPV16 irrespective of the ability of p53 to bind E2.

Even though the HFK+HPV16(-p53) cells had markers indicative of HPV16 immortalization, we noticed an aberrant growth phenotype in both foreskin donor cells (Fig. 6A and B). There was an initial enhanced proliferation of the HFK+HPV16(-p53) cells compared

with HFK+HPV16. However, around the 3–4 week mark, the HFK+HPV16(-p53) cells began to slow their growth and eventually stopped proliferating. To determine the mechanism of the attenuation of cell growth we investigated senescence in N/Tert-1, HFK+HPV16 and HFK+HPV16(-p53) cells by staining for beta-galactosidase following the end of the growth curve in donor 2 where the HFK+HPV16(-p53) had attenuated proliferation (day 40). There was a significantly increased number of senescent cells with the p53 mutant cells, and this was quantitated (Fig. 6C). Senescence can be induced by increased DNA damage, particularly double-strand breaks (DSB) (25, 26). Because CHK1 and CHK2 pathway activation was not noticeably different between HFK+HPV16 and HFK+HPV16 (-p53), we decided to look at DSBs more directly using single-cell gel electrophoresis (COMET assay) in low-passage-number HFK donor 2 cells. Because the HFK+HPV16(-p53) cells have attenuated proliferation at higher passage, we utilized early passage donor 2 cells corresponding to day 3 on the growth curve in Fig. 6A for these experiments. As expected, the expression of wild type or mutant HPV16 genomes in HFKs led to increased formation of DSBs as indicated by olive tail moment (OTM) compared to HPV negative N/Tert-1 cells (61) (Fig. 6D). However, the mutant HFKs consistently exhibited larger OTM values compared to HFK+HPV16 (Fig. 6D and E). As the expression of full-length E6 from a exogenous vector attenuates the growth of HFK+HPV16 wild-type cells (Fig. 2) we rationalized that expression of E6 should not alter the growth of HFK+HPV16(-p53) cells. Stable expression of exogenous full-length E6 or the E6Δp53 mutant had no additional effect on the proliferation of low-passage-number HFK+HPV16(-p53) cells, illustrating that the drastic differences in proliferation are likely due to the E2-p53 interaction (Fig. 6F).

HFK+HPV16(-p53) cells have an aberrant life cycle in differentiating epithelium. We organotypically rafted HFK+HPV16 and HFK+HPV16(-p53) cells. Both lines were placed on collagen plugs at early passage when the HFK+HPV16(-p53) cells retained proliferative capacity. Due to the large difference in growth rates between the wild type and mutant cells, the original plating was performed with both 1×10^6 and 2×10^6 cells to promote production of a monolayer on the collagen plugs prior to lifting to the liquid-air interface for differentiation. Fig. 7A demonstrates an aberrant differentiation process with the HFK+HPV16(-p53) cells compared with HFK+HPV16 cells at both cell densities. It is noticeable that at the lower cell density (1×10^6) there was a failure to form a monolayer prior to induction of differentiation (as evidenced by gaps between keratinocyte cell clusters on the collagen plug). Using a seeding density of 2×10^6 eliminated the formation of gaps but did not improve the proliferation. A representative of two independent donors is shown, both donors had identical phenotypes. Fig. 7B quantitates the results from two independent rafts from two independent donors; the mutant genomes have dramatically lower raft area compared with wild-type genomes. To investigate whether differentiation has occurred in these cells we stained with involucrin and keratin 10 (Fig. 7C). The mutant genome cells stained positive for both differentiation markers demonstrating that, even though raft growth is markedly attenuated, differentiation still occurs. We also stained for viral replication using the DNA-damage marker γ-H2AX. Recently we reported that an E2 mutant that failed to interact with TopBP1 results in degradation of E2 during organotypic rafting; this degradation would block viral replication and indeed these cells had no γ-H2AX staining (57). This demonstrates that the γ-H2AX staining indicates the occurrence of viral replication. Fig. 7D demonstrates that there is abundant nuclear γ-H2AX staining throughout HFK+HPV16 cells, indicating replication is occurring. The HFK+HPV16(-p53) cells also support viral replication although there is a reduction in the number of rafted cells stain positively for γ-H2AX (Fig. 7D).

DISCUSSION

The HPV E2 protein is essential for viral genome replication, segregation of viral episomes into daughter cells following cell division and can transcriptionally regulate both virus and host genomes (12, 19, 20). E2 interacts with a variety of host factors to promote progression of the viral life cycle, many of which are essential such as interactions with

TopBP1 and BRD4 (12, 19, 23, 55, 57). In this report, we propose that E2 binding to p53 is also an essential interaction as abrogation of the interaction leads to catastrophic failure of the viral life cycle.

In the classical high-risk HPV model, upon initial infection, the viral oncogenes E6 and E7 inhibit and degrade tumor suppressor proteins p53 and pRb, respectively, promoting hyperproliferation, unregulated DNA replication, mutation accumulation and potentially eventual carcinogenesis. Therefore, immortalization of cell lines can be achieved with overexpression vectors of E6 and E7 (Fig. 1A, Lanes 4 and 8). Previous studies suggest that E6 splice variants and their action on E6-E6AP-p53 complex disruption is cell cycle dependent (38). In HPV18 cell lines, E6*I shows marked upregulation and restored p53 expression during G2/M (38). We have previously illustrated that E2 is stabilized during mitosis which is important for its association with TopBP1 and its role as a segregation factor (57). It is entirely possible that the cell cycle mediated p53 restoration corresponds with E2 stabilization allowing these proteins to interact and could play an important role in genome segregation.

E2 can regulate host transcription in a multitude of ways. We recently reported that E2 can epigenetically repress the TWIST1 at the histone level, inhibiting EMT and promoting a less aggressive cellular phenotype (20). E2 can also promote the recruitment of DNA methyltransferase 1 to interferon response genes, resulting in DNA base methylation and global innate immunity downregulation (62). It is currently unclear how E2 recruits epigenetic modifiers to these genes and p53 may play an important role. DNA methyltransferases (DMNTs) are often part of large multimeric complexes and use transcription regulatory proteins to help target specific genes undergoing epigenetic silencing (63, 64). p53 is known to also interact with DMNT1 resulting in the methylation of antiapoptotic genes (65). It is possible that the interaction between E2 and p53 is important for the rerouting of DNMTs to different genes whose regulation is important for a healthy viral life cycle. It is also noticeable that the mutant E2 has an attenuated ability to activate transcription (Fig. 3), indicating that regulation of host gene transcription by E2 may require co-operation with p53 in some cases.

These mutations in E2 would also potentially prevent interaction of p53 with E8^E2. This protein controls replication of episomal viral genomes and p53 may play a role in this E8^E2 function that is disrupted by the p53 interaction mutations (66–70). Future studies will focus on determining whether the E8^E2 interaction with p53 regulates the function of the viral protein.

The results from Fig. 6D suggest that additional double-strand breaks play a role in the enhanced damage and proliferation rate of HFK+HPV16(-p53) mutant cells compared to wild type immortalized HFKs. HPV uses homologous recombination (HR) factors to assist in viral replication (71–73). Conversely, p53 binds to replication protein A (RPA) resulting in repression of HR, reducing DSB repair and promoting apoptosis during catastrophic genome instability (27, 29). It is possible that E2 helps regulate this activity of p53 and inability to do so results in accumulation of DSBs as seen in Fig. 6D.

In conclusion, this report indicates that p53 expression is retained in HPV16 positive cell lines and tumor samples under a variety of conditions. Knockdown of this residual p53 by full-length E6 results in significant reduction in proliferation and enhanced senescence in cells immortalized with HPV16 which we attribute to loss of E2 interaction with p53. Human foreskin cells immortalized by HPV16 where E2 can no longer bind to p53 exhibit aberrant phenotypes, including dysregulated proliferation, enhanced levels of DSBs and overall failure of the viral life cycle during organotypic raft culturing. Due to the importance of p53 in the context of HPV related cancers as well as the profound phenotypes demonstrated in this report, further investigation on the interaction between E2 and p53 is warranted.

MATERIALS AND METHODS

Cell culture. N/Tert-1 cells and head-and-neck cancer lines UMSCC47 and UMSCC104 were cultured as previously described (20, 62, 74–76). Immortalization and culturing of human foreskin keratinocytes with HPV16 are described below. All cell lines were grown as pools, incubated at 37°C and 5% CO2 with

media changed every 3 days. For cisplatin treatment, cells were incubated with indicated concentrations of drug dissolved in DMF or DMF vehicle control for 24-h.

Immortalization of human foreskin keratinocytes (HFK). The HPV16 mutant genome (HPV16 [-p53], which contained an E2 unable to bind p53) was generated and sequenced by Genscript (42, 44, 77). Residues Aspartic acid 388, Tryptophan 341 and Aspartic acid 344 were all mutated to alanine resulting in inability for E2 to interact with p53 in a similar method to the generation of the E2(-p53) plasmid as described below. The HPV16 genome was removed from the parental plasmid using *SphI*, and the viral genomes isolated and then recircularized using T4 ligase (NEB) and transfected into early passage HFK from three donor backgrounds (Lifeline technology), alongside a G418 resistance plasmid, pcDNA. Cells underwent selection in 200 μg/mL G418 (Sigma-Aldrich) for 14 days and were cultured on a layer of J2 3T3 fibroblast feeders (NIH), which had been pretreated with 8 μg/mL mitomycin C (Roche). Throughout the immortalization process, HFK were cultured in Dermalife-K complete media (Lifeline Technology). The experiments in Fig. 6B to F were performed using donor 2.

Western blotting. Protein from cell pellets was extracted with 2× pellet volume protein lysis buffer (0.5% Nonidet P-40, 50 mM Tris [pH 7.8], and 150 mM NaCl) supplemented with protease inhibitor (Roche Molecular Biochemicals) and phosphatase inhibitor cocktail (Sigma). Protein extraction from patient derived xenografts was performed as previously described (45, 46). The cells were lysed on ice for 30 min followed by centrifugation at 18,000 rcf (relative centrifugal force) for 20 min at 4°C. Protein concentration was estimated colorimetrically using a Bio-Rad protein assay and 25 μg of protein with equal volume of 2× Laemmli sample buffer (Bio-Rad) was denatured at 70°C for 10 min. The samples were run on a Novex WedgeWell 4% to 12% Tris-glycine gel (Invitrogen) and transferred onto a nitrocellulose membrane (Bio-Rad) using the wet-blot method, at 30 V overnight. The membrane was blocked with *Li-Cor* Odyssey blocking buffer (PBS) diluted 1:1 vol/vol with PBS for 1 h at room temperature and then incubated with specified primary antibody in *Li-Cor* Odyssey blocking buffer (PBS) diluted 1:1 with PBS. Afterwards, the membrane was washed with PBS supplemented with 0.1% Tween20 and further probed with the Odyssey secondary antibodies (IRDye 680RD Goat anti-Rabbit IgG (H+L), 0.1 mg or IRDye 800CW Goat anti-Mouse IgG (H+L), 0.1 mg) in *Li-Cor* Odyssey blocking buffer (PBS) diluted 1:1 with PBS at 1:10,000 for 1 h at room temperature where applicable. After washing with PBS-Tween, the membrane was imaged using the Odyssey CLx Imaging System and ImageJ was used for quantification. Primary antibodies used for Western blotting studies are as follows: p53, 1:1000 (Santa Cruz; cat. no. sc-47698) HPV16 E2, 1:1000 (TVG261) (Abcam; cat. no. ab17185) phospho-CHK1, 1:1000 (Ser345) (Cell Signaling; cat. No. 2341S), phosphor CHK2 (Thr68), 1:1000 (Cell Signaling; cat. No. 2661S), CHK1, 1:1000 (Cell Signaling; cat. No. 2360), CHK2, 1:1000 (Abcam; cat. No. ab47443), GAPDH, 1:250 (Santa Cruz; cat. no. sc-47724).

Plasmids. The following plasmids were used the completion of these studies: pMSCV-N-FLAG-HA-GFP, pMSCV-N-FLAG-HA-HPV16E6, pMSCV-IP-N-FLAG-HA-16E6 8S9A10T ("E6Δp53") where residues Arg 8, Pro 9 and Arg 10 are replaced with Ser, Ala and Thr, respectively. Wild-type 16E2 (E2-WT) or E2(-p53) (Mutated residues W341A, D344A, D338A) were cloned into pcDNA3.0 vector for confirmation of p53 interaction in N/Tert-1 cells. pcDNA3.0 was used for empty vector control.

Real-time qPCR. RNA was isolated using the SV Total RNA isolation system (Promega) according to manufacturer's instructions. 2 μg of RNA was reverse transcribed into cDNA using the high-capacity reverse transcription kit (Applied Biosystems). The PowerUp SYBR green master mix (Applied Biosystems) was used along with cDNA and gene specific primers and real-time PCR was performed using a 7500 Fast real-time PCR system as previously described. (20, 62, 74). Expression was quantified as relative quantity over GAPDH using the $2^{-\Delta\Delta C_T}$ method. Primers used are as follows. FLAG-HA Tag fwd 5′- GACTACAAGGATGACGATG- 3′, FLAG-HA Tag rev 5′- GCGTAATCTGGAACATCG -3′.

Immunoprecipitation. Primary polyclonal antibody against p53 (Invitrogen; PA5-27822) or a HA-tag antibody (used as a negative control) was incubated in 200 μg of cell lysate (prepared as described above), made up to a total volume of 500 μL with lysis buffer (0.5% Nonidet P-40, 50 mM Tris [pH 7.8], and 150 mM NaCl), supplemented with protease inhibitor (Roche Molecular Biochemicals) and phosphatase inhibitor cocktail (Sigma) and rotated at 4°C overnight. The following day, 50 μL of prewashed protein A-Sepharose beads per sample was added to the lysate/antibody solution and rotated for 4 h at 4°C. The samples were gently washed with 500 μL lysis buffer by centrifugation at 1,000 rcf for 2–3 min. This wash was repeated 4 times. The bead pellet was resuspended in 4× Laemmli sample buffer (Bio-Rad), heat denatured and centrifuged at 1,000 rcf for 2–3 min. Proteins were separated using an SDS-PAGE system and transferred onto a nitrocellulose membrane before probing for the presence of E2 or p53, as per Western blotting protocol. For the E1-E2 immunoprecipitation in Fig. 1 and 3, μg HA-HPV16E1 was transfected into U2OS cells stably expressing E2, E2(-p53) or empty vector. 48h later, the cells were harvested for protein as described above and anti-HA was used to co-immunoprecipitate E2 with HA-E1. Anti-FLAG antibody was used for negative antibody control in this experiment.

Transcription and LCR repression assays. A ptk6E2-Luciferase reporter plasmid was utilized to analyze transcriptional activation of Wild-type HPV16 E2 (E2-WT) and E2(-p53) proteins as previously described (23). 5×10^5 N/Tert-1 cells were seeded onto 100mm^2 plate and transfected 24 h later with 0 ng, 10 ng, 100 ng or 1000 ng of E2 WT or E2(-p53) plasmid DNA along with 1000 ng of ptk6E2-Luciferase reporter plasmid using Lipofectamine 2000 according to the manufacturer's instructions (ThermoFisher Scientific). Cells were harvested the next day using Promega luciferase assay system. For LCR repression activity, a pHPV16-LCR-Luciferase reporter was used in place of the ptk6E2-Luciferase plasmid (74).

Chromatin immunoprecipitation. N/tert-1 cells expressing either pcDNA3.0 (vector control), wild-type E2 (E2-WT) or E2(-p53) were transfected with 1 μg of pHPV16LCR-luc or 1 μg of pTK6E2-luc, using a

Lipofectamine method (SigmaAldrich). The following day, cells were transferred to 15-cm^2 dishes. At 48 h posttransfection, cells were washed twice with cold PBS and then cross-linked with 1% formaldehyde at room temperature for 15 min. The cross-linking reaction was stopped using 0.125 M glycine, and cells lysed by scraping and incubation on ice in 1.5 cell pellet volume of cell lysis buffer (10 mM Tris-HCl, pH 8.0, 10 mM NaCl, 0.2% NP-40, 10 mM sodium butyrate, 50 g/mL phenylmethylsulfonyl fluoride [PMSF], 1× complete protease inhibitor). After 10 min, nuclei were collected by centrifugation at 2,500 rpm at 4°C. Nuclei were lysed by resuspension in 1.2 mL of nuclear lysis buffer (50 mM Tris-HCl, pH 8.1, 10 mM EDTA, 1% SDS, 10 mM sodium butyrate, 50 g/mL PMSF, 1× complete protease inhibitor), and incubation on ice for 10 min. This was then diluted in 0.72 mL of immunoprecipitation dilution buffer (IPDB; 20 mM Tris-HCl, pH 8.1, 150 mM NaCl, 2 mM EDTA, 1% Triton X-100, 0.01% SDS, 10 mM sodium butyrate, 50 g/mL PMSF, 1× complete protease inhibitor). Chromatin was sheared using a water bath sonicator (Diagenode Bioruptor 300). 100 μg of chromatin was incubated with 2 μg sheep anti-HPV16 E2 antibody (54) and 20 μL of a slurry of A/G magnetic beads (prewashed in IPDB) (Thermo Fisher Scientific; product number 26162) with rotation at 4°C overnight. The following day, beads were washed twice withIP wash buffer 1 (20 mM Tris-HCl, pH 8.1, 50 mM NaCl, 2 mM EDTA, 1% Triton X-100, 0.1% SDS) and then twice with IP wash buffer 2 (10 mM Tris-HCl, pH 8.1, 250 mM LiCl, 1 mM EDTA, 1% NP-40, 1% deoxycholic acid) and, finally, washed twice with Tris-EDTA (TE), pH 8.0. The immune complexes were eluted from the beads by addition of IP elution buffer (IPEB; 100 mM NaHCO3, 1% SDS) and 10 μg RNase A, altogether incubated at 65°C for 30 min. Beads were then magnetically separated from the supernatant, leaving the chromatin immunoprecipitation (ChIP) DNA, which was incubated for 6 h at 65°C. To digest the immune complexes, 100 μg of proteinase K was added and incubated overnight at 45°C. DNA was then purified using the phenol chloroform method and qRT-PCR carried out on the resulting DNA using primers corresponding to luciferase (Fwd 5′-CTCACTGAGACTACATCAGC-3′, Rev 5′-TCCAGATCCACAACCTTCGC-3′ Rev) and TWIST1 promoter (20).

Southern blotting. Total cellular DNA was extracted by proteinase K-sodium dodecyl sulfate digestion followed by a phenol-chloroform extraction method. 5 μg of total cellular DNA was digested with either SphI (to linearize the HPV16 genome) or HindIII (which fails to cut HPV16 genome). All digestions included DpnI to ensure that all input DNA was digested. All restriction enzymes were purchased from NEB and utilized as per manufacturer's instructions. Digested DNA was separated by electrophoresis of a 0.8% agarose gel, transferred to a nitrocellulose membrane, and probed with radiolabeled (32-P) HPV16 genome as previously described. This was then visualized by exposure to film for 1 to 24 h. Images were captured from an overnight-exposed phosphor screen by GE Typhoon 9410 and quantified using ImageJ.

Exonuclease V assay. PCR based analysis of viral genome status was performed using methods described by Myers et al. (59). Briefly, 20 ng genomic DNA was either treated with exonuclease V (RecBCD, NEB), in a total volume of 30 μL, or left untreated for 1 h at 37°C followed by heat inactivation at 95°C for 10 min. 2 ng of digested/undigested DNA was then quantified by real-time PCR using a 7500 FAST Applied Biosystems thermocycler with SYBR green PCR Master Mix (Applied Biosystems) and 100 nM primer in a 20 μL reaction. Nuclease free water was used in place of the template for a negative control. The following cycling conditions were used: 50°C for 2 min, 95°C for 10 min, 40 cycles at 95°C for 15 s, and a dissociation stage of 95°C for 15 s, 60°C for 1 min, 95°C for 15 s, and 60°C for 15 s. Separate PCRs were performed to amplify HPV16 E6 F: 5′- TTGCTTTTCGGGATTTATGC-3′ R: 5′- CAGGACACAGTGGCTTTTGA-3′, HPV16 E2 F: 5′-TGGAAGTGCAGTTTGATGGA-3′ R: 5′-CCGCATGAACTTCCCATACT-3′, human mitochondrial DNA F: 5′-CAGGAGTAGGAGAGAGGGAGGTAAG-3′ R: 5′-TACCCATCATAATCGGAGGCTTTGG -3′, and human GAPDH DNA F: 5′-GGAGCGAGATCCCTCCAAAAT-3′ R: 5′-GGCTGTTGTCATACTTCTCATGG-3′

Senescence staining. 7.5 × 10^4 cells were seeded in 6-well plates. The following day, cells were stained for senescence using the Cell Signal Senescence β-Galactosidase Staining kit according to manufacturer's instructions (9860). Randomly selected images were taken using the Keyence imaging system at 10×. Positively stained cells were counted by a blinded observer and average number of positively stained cells per field were calculated. The senescence staining in Fig. 2C corresponds with day 11 on the growth curve in 2 A/B. In Fig. 6, HFK lines were stained at the last point in the growth curve in donor 2 which was day 40.

Single-cell gel electrophoresis (COMET) assay. 1 × 10^4 cells were plated in 24-well plate with 1 mL media 1 day prior to harvest. The next day, cells were trypsinized and resuspended in a mixture 0.5% wt/vol Low molecular weight agarose (Lonza, cat. No. #50101) and PBS at a ratio of 10:1. Suspension was immediately pipetted onto Trivegen COMET Slides^{TM} (4250-004-03) and allowed to dry for 30 min at 4°C. Slides underwent lysis for 90 min at 4°C in the dark (Lysis buffer: 10 mM Tris, 100 mM EDTA, 2.5 M NaCl, 1% TritonX100, 10%DMSO titrated to pH 10.0). Afterwards slides were placed in Alkaline buffer for 25 min at 4°C in the dark (Alkaline buffer: 1 mM EDTA, 200 mM NaOH, pH >13.0). Slides were transferred to an agarose gel electrophoresis box filled with additional alkaline buffer. Electrophoresis was performed at 25V for 20 min at room temperature in the dark. Slides were then washed 2× in dd (double distilled) H2O for 5 min at RT and then placed in neutralization buffer for 20 min at RT in dark (Neutralization buffer: 400 mM Tris-HCl titrated to pH 7.5). Neutralized slides were then left to dry at 37°C in the dark. Dried slides were stained with DAPI (1:10,000 in dd H2O) for 15 min at RT then washed 2× with dd H_2O for 5 min. Stained and rinsed slides were left to dry overnight. Slides were imaged using the Keyence imaging system at 20× with >5 images taken per replicate. Quantization of olive tail moments (OTM) was achieved using the CASPLab COMET Assay imaging software by Końca K et al., 2003 (78).

Organotypic raft culture. Keratinocytes were differentiated via organotypic raft culture as described previously (62, 76, 79). Briefly, cells were seeded onto type 1 collagen matrices containing J2 3T3

fibroblast feeder cells. Cells were cultured to confluence atop the collagen plugs, lifted onto wire grids and cultured in cell culture dishes at the air-liquid interface. Media was replaced on alternating days. Following 14 days of culture, rafted samples were fixed with formaldehyde (4% vol/vol) and embedded in paraffin. Multiple 4 μm sections were cut from each sample. Sections were stained with hematoxylin and eosin (H&E) and others prepared for immunofluorescent staining via HIER. Fixing and embedding services in support of the research project were generated by the VCU Massey Cancer Center Cancer Mouse Model Shared Resource, supported, in part, with funding from NIH-NCI Cancer Center Support Grant P30 CA016059. Fixed sections were antigen retrieved in citrate buffer and probed with the following antibodies for immunofluorescent anaylsis: phospho-yH2AX 1/500 (Cell Signaling Technology; 9718), Involucrin 1/1000 (abcam; ab27495), and Keratin 10 1/1000 (SigmaAldrich; SAB4501656). Cellular DNA was stained with 4′,6-diamidino-2-phenylindole (DAPI, Santa Cruz sc-3598). Microscopy was performed using the Keyence imaging system,

ACKNOWLEDGMENTS

This work was supported by VCU Philips Institute for Oral Health Research and the National Cancer Institute designated Massey Cancer Center grant P30 CA016059 (I.M.M.). D.B. is supported by R01DE027185, a grant from the National Institute of Dental and Craniofacial Research.

REFERENCES

1. Zur Hausen H. 2009. Papillomaviruses in the causation of human cancers - a brief historical account. Virology 384:260–265. https://doi.org/10.1016/j.virol.2008.11.046.
2. Marur S, D'Souza G, Westra WH, Forastiere AA. 2010. HPV-associated head and neck cancer: a virus-related cancer epidemic. Lancet Oncol 11:781–789. https://doi.org/10.1016/S1470-2045(10)70017-6.
3. Gillison ML, Koch WM, Capone RB, Spafford M, Westra WH, Wu L, Zahurak ML, Daniel RW, Viglione M, Symer DE, Shah KV, Sidransky D. 2000. Evidence for a causal association between human papillomavirus and a subset of head and neck cancers. J Natl Cancer Inst 92:709–720. https://doi.org/10.1093/jnci/92.9.709.
4. Gillison ML. 2004. Human papillomavirus-associated head and neck cancer is a distinct epidemiologic, clinical, and molecular entity. Semin Oncol 31:744–754. https://doi.org/10.1053/j.seminoncol.2004.09.011.
5. Chaturvedi AK, Engels EA, Pfeiffer RM, Hernandez BY, Xiao W, Kim E, Jiang B, Goodman MT, Sibug-Saber M, Cozen W, Liu L, Lynch CF, Wentzensen N, Jordan RC, Altekruse S, Anderson WF, Rosenberg PS, Gillison ML. 2011. Human papillomavirus and rising oropharyngeal cancer incidence in the United States. JCO 29:4294–4301. https://doi.org/10.1200/JCO.2011.36.4596.
6. Thierry F. 2009. Transcriptional regulation of the papillomavirus oncogenes by cellular and viral transcription factors in cervical carcinoma. Virology 384:375–379. https://doi.org/10.1016/j.virol.2008.11.014.
7. Scheffner M, Huibregtse JM, Vierstra RD, Howley PM. 1993. The HPV-16 E6 and E6-AP complex functions as a ubiquitin-protein ligase in the ubiquitination of p53. Cell 75:495–505. https://doi.org/10.1016/0092-8674(93)90384-3.
8. Mittal S, Banks L. 2017. Molecular mechanisms underlying human papillomavirus E6 and E7 oncoprotein-induced cell transformation. Mutat Res Rev Mutat Res 772:23–35. https://doi.org/10.1016/j.mrrev.2016.08.001.
9. Huibregtse JM, Scheffner M, Howley PM. 1991. A cellular protein mediates association of p53 with the E6 oncoprotein of human papillomavirus types 16 or 18. EMBO J 10:4129–4135. https://doi.org/10.1002/j.1460-2075.1991.tb04990.x.
10. Thomas M, Pim D, Banks L. 1999. The role of the E6-p53 interaction in the molecular pathogenesis of HPV. Oncogene 18:7690–7700. https://doi.org/10.1038/sj.onc.1202953.
11. Hoppe-Seyler K, Bossler F, Braun JA, Herrmann AL, Hoppe-Seyler F. 2018. The HPV E6/E7 Oncogenes: key Factors for Viral Carcinogenesis and Therapeutic Targets. Trends Microbiol 26:158–168. https://doi.org/10.1016/j.tim.2017.07.007.
12. McBride AA. 2013. The Papillomavirus E2 proteins. Virology 445:57–79. https://doi.org/10.1016/j.virol.2013.06.006.
13. Loo YM, Melendy T. 2004. Recruitment of replication protein A by the papillomavirus E1 protein and modulation by single-stranded DNA. J Virol 78:1605–1615. https://doi.org/10.1128/jvi.78.4.1605-1615.2004.
14. Bergvall M, Melendy T, Archambault J. 2013. The E1 proteins. Virology 445:35–56. https://doi.org/10.1016/j.virol.2013.07.020.
15. Stanley MA, Pett MR, Coleman N. 2007. HPV: from infection to cancer. Biochem Soc Trans 35:1456–1460. https://doi.org/10.1042/BST0351456.
16. Stanley MA. 2012. Epithelial cell responses to infection with human papillomavirus. Clin Microbiol Rev 25:215–222. https://doi.org/10.1128/CMR.05028-11.
17. Doorbar J, Quint W, Banks L, Bravo IG, Stoler M, Broker TR, Stanley MA. 2012. The biology and life-cycle of human papillomaviruses. Vaccine 30 Suppl 5:F55–70. https://doi.org/10.1016/j.vaccine.2012.06.083.
18. Bouvard V, Storey A, Pim D, Banks L. 1994. Characterization of the human papillomavirus E2 protein: evidence of trans-activation and trans-repression in cervical keratinocytes. EMBO J 13:5451–5459. https://doi.org/10.1002/j.1460-2075.1994.tb06880.x.
19. McBride AA, Sakakibara N, Stepp WH, Jang MK. 2012. Hitchhiking on host chromatin: how papillomaviruses persist. Biochim Biophys Acta 1819:820–825. https://doi.org/10.1016/j.bbagrm.2012.01.011.
20. Fontan CT, Das D, Bristol ML, James CD, Wang X, Lohner H, Atfi A, Morgan IM. 2020. Human papillomavirus 16 E2 repression of TWISTI transcrption is a potential mediator of HPV16 cancer outcomes. MSphere 5. https://doi.org/10.1128/mSphere.00981-20.
21. Gauson EJ, Windle B, Donaldson MM, Caffarel MM, Dornan ES, Coleman N, Herzyk P, Henderson SC, Wang X, Morgan IM. 2014. Regulation of human genome expression and RNA splicing by human papillomavirus 16 E2 protein. Virology 468-470:10–18. https://doi.org/10.1016/j.virol.2014.07.022.
22. Evans MR, James CD, Bristol ML. 2019. Human papillomavirus 16 E2 regulates keratinocyte gene expression relevant to cancer and the viral life cycle. 93.
23. Gauson EJ, Wang X, Dornan ES, Herzyk P, Bristol M, Morgan IM. 2016. Failure to interact with Brd4 alters the ability of HPV16 E2 to regulate host genome expression and cellular movement. Virus Res 211:1–8. https://doi.org/10.1016/j.virusres.2015.09.008.
24. Muller M, Demeret C. 2012. The HPV E2-host protein-protein interactions: a complex hijacking of the cellular network. Open Virol J 6:173–189. https://doi.org/10.2174/1874357901206010173.
25. Yee KS, Vousden KH. 2005. Complicating the complexity of p53. Carcinogenesis 26:1317–1322. https://doi.org/10.1093/carcin/bgi122.
26. Vousden KH, Lane DP. 2007. p53 in health and disease. Nat Rev Mol Cell Biol 8:275–283. https://doi.org/10.1038/nrm2147.
27. Romanova LY, Willers H, Blagosklonny MV, Powell SN. 2004. The interaction of p53 with replication protein A mediates suppression of homologous recombination. Oncogene 23:9025–9033. https://doi.org/10.1038/sj.onc.1207982.
28. Lane DP. 1992. Cancer. p53, guardian of the genome. Nature 358:15–16. https://doi.org/10.1038/358015a0.
29. Gatz SA, Wiesmüller L. 2006. p53 in recombination and repair. Cell Death Differ 13:1003–1016. https://doi.org/10.1038/sj.cdd.4401903.
30. Cheng Q, Chen J. 2010. Mechanism of p53 stabilization by ATM after DNA damage. Cell Cycle 9:472–478. https://doi.org/10.4161/cc.9.3.10556.
31. Li S, Hong X, Wei Z, Xie M, Li W, Liu G, Guo H, Yang J, Wei W, Zhang S. 2019. Ubiquitination of the HPV Oncoprotein E6 Is Critical for E6/E6AP-Mediated p53 Degradation. Front Microbiol 10:2483–2483. https://doi.org/10.3389/fmicb.2019.02483.

32. Vande Pol SB, Klingelhutz AJ. 2013. Papillomavirus E6 oncoproteins. Virology 445:115–137. https://doi.org/10.1016/j.virol.2013.04.026.
33. Martinez-Zapien D, Ruiz FX, Poirson J, Mitschler A, Ramirez J, Forster A, Cousido-Siah A, Masson M, Vande Pol S, Podjarny A, Travé G, Zanier K. 2016. Structure of the E6/E6AP/p53 complex required for HPV-mediated degradation of p53. Nature 529:541–545. https://doi.org/10.1038/nature16481.
34. Zhou G, Liu Z, Myers JN. 2016. TP53 mutations in head and neck squamous cell carcinoma and their impact on disease progression and treatment response. J Cell Biochem 117:2682–2692. https://doi.org/10.1002/jcb.25592.
35. Poeta ML, Manola J, Goldwasser MA, Forastiere A, Benoit N, Califano JA, Ridge JA, Goodwin J, Kenady D, Saunders J, Westra W, Sidransky D, Koch WM. 2007. TP53 mutations and survival in squamous-cell carcinoma of the head and neck. N Engl J Med 357:2552–2561. https://doi.org/10.1056/NEJMoa073770.
36. Pim D, Massimi P, Banks L. 1997. Alternatively spliced HPV-18 E6* protein inhibits E6 mediated degradation of p53 and suppresses transformed cell growth. Oncogene 15:257–264. https://doi.org/10.1038/sj.onc.1201202.
37. Smotkin D, Wettstein FO. 1986. Transcription of human papillomavirus type 16 early genes in a cervical cancer and a cancer-derived cell line and identification of the E7 protein. Proc Natl Acad Sci U S A 83:4680–4684. https://doi.org/10.1073/pnas.83.13.4680.
38. Guccione E, Pim D, Banks L. 2004. HPV-18 E6*I modulates HPV-18 full-length E6 functions in a cell cycle dependent manner. Int J Cancer 110:928–933. https://doi.org/10.1002/ijc.20184.
39. Schneider-Gädicke A, Schwarz E. 1986. Different human cervical carcinoma cell lines show similar transcription patterns of human papillomavirus type 18 early genes. EMBO J 5:2285–2292. https://doi.org/10.1002/j.1460-2075.1986.tb04496.x.
40. Kösel S, Burggraf S, Engelhardt W, Olgemöller B. 2007. Increased levels of HPV16 E6*I transcripts in high-grade cervical cytology and histology (CIN II+) detected by rapid real-time RT-PCR amplification. Cytopathology 18:290–299. https://doi.org/10.1111/j.1365-2303.2007.00481.x.
41. Nulton TJ, Olex AL, Dozmorov M, Morgan IM, Windle B. 2017. Analysis of The Cancer Genome Atlas sequencing data reveals novel properties of the human papillomavirus 16 genome in head and neck squamous cell carcinoma. Oncotarget 8:17684–17699. https://doi.org/10.18632/oncotarget.15179.
42. Webster K, Parish J, Pandya M, Stern PL, Clarke AR, Gaston K. 2000. The human papillomavirus (HPV) 16 E2 protein induces apoptosis in the absence of other HPV proteins and via a p53-dependent pathway. J Biol Chem 275:87–94. https://doi.org/10.1074/jbc.275.1.87.
43. Parish JL, Kowalczyk A, Chen HT, Roeder GE, Sessions R, Buckle M, Gaston K. 2006. E2 proteins from high- and low-risk human papillomavirus types differ in their ability to bind p53 and induce apoptotic cell death. J Virol 80:4580–4590. https://doi.org/10.1128/JVI.80.9.4580-4590.2006.
44. Brown C, Kowalczyk A, Taylor E, Morgan I, Gaston K. 2008. P53 represses human papillomavirus type 16 DNA replication via the viral E2 protein. Virol J 5:5. https://doi.org/10.1186/1743-422X-5-5.
45. Facompre ND, Sahu V, Montone KT, Harmeyer KM, Nakagawa H, Rustgi AK, Weinstein GS, Gimotty PA, Basu D. 2017. Barriers to generating PDX models of HPV-related head and neck cancer. Laryngoscope 127:2777–2783. https://doi.org/10.1002/lary.26679.
46. Facompre ND, Rajagopalan P, Sahu V, Pearson AT, Montone KT, James CD, Gleber-Netto FO, Weinstein GS, Jalaly J, Lin A, Rustgi AK, Nakagawa H, Califano JA, Pickering CR, White EA, Windle BE, Morgan IM, Cohen RB, Gimotty PA, Basu D. 2020. Identifying predictors of HPV-related head and neck squamous cell carcinoma progression and survival through patient-derived models. https://doi.org/10.1002/ijc.33125.
47. Friedel L, Loewer A. 2022. The guardian's choice: how p53 enables context-specific decision-making in individual cells. FEBS J 289:40–52. https://doi.org/10.1111/febs.15767.
48. Suton P, Skelin M, Rakusic Z, Dokuzovic S, Luksic I. 2019. Cisplatin-based chemoradiotherapy vs. cetuximab-based bioradiotherapy for p16-positive oropharyngeal cancer: an updated meta-analysis including trials RTOG 1016 and De-ESCALaTE. Eur Arch Otorhinolaryngol 276:1275–1281. https://doi.org/10.1007/s00405-019-05387-8.
49. Gillison ML, Trotti AM, Harris J, Eisbruch A, Harari PM, Adelstein DJ, Jordan RCK, Zhao W, Sturgis EM, Burtness B, Ridge JA, Ringash J, Galvin J, Yao M, Koyfman SA, Blakaj DM, Razaq MA, Colevas AD, Beitler JJ, Jones CU, Dunlap NE, Seaward SA, Spencer S, Galloway TJ, Phan J, Dignam JJ, Le QT. 2019. Radiotherapy plus cetuximab or cisplatin in human papillomavirus-positive oropharyngeal cancer (NRG Oncology RTOG 1016): a randomised, multicentre, non-inferiority trial. Lancet 393:40–50. https://doi.org/10.1016/S0140-6736(18)32779-X.
50. Mehanna H, Robinson M, Hartley A, Kong A, Foran B, Fulton-Lieuw T, Dalby M, Mistry P, Sen M, O'Toole L, Al Booz H, Dyker K, Moleron R, Whitaker S, Brennan S, Cook A, Griffin M, Aynsley E, Rolles M, De Winton E, Chan A, Srinivasan D, Nixon I, Grumett J, Leemans CR, Buter J, Henderson J, Harrington K, McConkey C, Gray A, Dunn J, Moleron R, McArdle O, Dyker K, Al Booz H, O'Toole L, Cook A, Husband D, Loo V, Soe W, Aynsley E, Sridhar T, Jankowska P, Joseph M, Geropantas K, Vaidya D, Griffin M, Hartley A, Vijayan R, Hwang D, et al. 2019. Radiotherapy plus cisplatin or cetuximab in low-risk human papillomavirus-positive oropharyngeal cancer (De-ESCALaTE HPV): an open-label randomised controlled phase 3 trial. Lancet 393:51–60. https://doi.org/10.1016/S0140-6736(18)32752-1.
51. Jeremic B, Shibamoto Y, Stanisavljevic B, Milojevic L, Milicic B, Nikolic N. 1997. Radiation therapy alone or with concurrent low-dose daily either cisplatin or carboplatin in locally advanced unresectable squamous cell carcinoma of the head and neck: a prospective randomized trial. Radiother Oncol 43:29–37. https://doi.org/10.1016/s0167-8140(97)00048-0.
52. Scarth JA, Patterson MR, Morgan EL, Macdonald A. 2021. The human papillomavirus oncoproteins: a review of the host pathways targeted on the road to transformation. J Gen Virol 102. https://doi.org/10.1099/jgv.0.001540.
53. Kiyono T, Foster SA, Koop JI, McDougall JK, Galloway DA, Klingelhutz AJ. 1998. Both Rb/p16INK4a inactivation and telomerase activity are required to immortalize human epithelial cells. Nature 396:84–88. https://doi.org/10.1038/23962.
54. Das D, Smith N, Wang X, Morgan IM. 2017. The Deacetylase SIRT1 Regulates the Replication Properties of Human Papillomavirus 16 E1 and E2. J Virol 91:e00102-17. https://doi.org/10.1128/JVI.00102-17.
55. Gauson EJ, Donaldson MM, Dornan ES, Wang X, Bristol M, Bodily JM, Morgan IM. 2015. Evidence supporting a role for TopBP1 and Brd4 in the initiation but not continuation of human papillomavirus 16 E1/E2 mediated DNA replication. J Virol 89:17684–17699. https://doi.org/10.1128/JVI.00335-15.
56. Boner W, Taylor ER, Tsirimonaki E, Yamane K, Campo MS, Morgan IM. 2002. A Functional interaction between the human papillomavirus 16 transcription/replication factor E2 and the DNA damage response protein TopBP1. J Biol Chem 277:22297–22303. https://doi.org/10.1074/jbc.M202163200.
57. Prabhakar AT, James CD, Das D, Otoa R, Day M, Burgner J, Fontan CT, Wang X, Glass SH, Wieland A, Donaldson MM, Bristol ML, Li R, Oliver AW, Pearl LH, Smith BO, Morgan IM. 2021. CK2 phosphorylation of human papillomavirus 16 E2 on Serine 23 promotes interaction with TopBP1 and is critical for E2 interaction with mitotic chromatin and the viral life cycle. mBio 12:e0116321. https://doi.org/10.1128/mBio.01163-21:e0116321.
58. Myers JE, Zwolinska K, Sapp MJ, Scott RS. 2020. An exonuclease V-qPCR assay to analyze the state of the human papillomavirus 16 genome in cell lines and tissues. Curr Protoc Microbiol 59:e119.
59. Myers JE, Guidry JT, Scott ML, Zwolinska K, Raikhy G, Prasai K, Bienkowska-Haba M, Bodily JM, Sapp MJ, Scott RS. 2019. Detecting episomal or integrated human papillomavirus 16 DNA using an exonuclease V-qPCR-based assay. Virology 537:149–156. https://doi.org/10.1016/j.virol.2019.08.021.
60. James CD, Fontan CT, Otoa R, Das D, Prabhakar AT, Wang X, Bristol ML, Morgan IM. 2020. Human papillomavirus 16 E6 and E7 synergistically repress innate immune gene transcription. mSphere 5. https://doi.org/10.1128/mSphere.00828-19.
61. Mehta K, Laimins L. 2018. Human papillomaviruses preferentially recruit DNA repair factors to viral genomes for rapid repair and amplification. mBio 9:e00064-18. https://doi.org/10.1128/mBio.00064-18.
62. Evans MR, James CD, Bristol ML, Nulton TJ, Wang X, Kaur N, White EA, Windle B, Morgan IM. 2019. Human papillomavirus 16 E2 regulates keratinocyte gene expression relevant to cancer and the viral life cycle. J Virol 93:e01941-18. https://doi.org/10.1128/JVI.01067-19.
63. Dahlet T, Argüeso Lleida A, Al Adhami H, Dumas M, Bender A, Ngondo RP, Tanguy M, Vallet J, Auclair G, Bardet AF, Weber M. 2020. Genome-wide analysis in the mouse embryo reveals the importance of DNA methylation for transcription integrity. Nat Commun 11:3153–3153. https://doi.org/10.1038/s41467-020-16919-w.
64. Smith ZD, Meissner A. 2013. DNA methylation: roles in mammalian development. Nat Rev Genet 14:204–220. https://doi.org/10.1038/nrg3354.
65. Estève P-O, Chin HG, Pradhan S. 2005. Human maintenance DNA (cytosine-5)-methyltransferase and p53 modulate expression of p53-repressed promoters. Proc Natl Acad Sci U S A 102:1000–1005. https://doi.org/10.1073/pnas.0407729102.

66. Dreer M, Fertey J, van de Poel S, Straub E, Madlung J, Macek B, Iftner T, Stubenrauch F. 2016. Interaction of NCOR/SMRT repressor complexes with papillomavirus E8^E2C proteins inhibits viral replication. PLoS Pathog 12:e1005556. https://doi.org/10.1371/journal.ppat.1005556.
67. Straub E, Dreer M, Fertey J, Iftner T, Stubenrauch F. 2014. The viral E8^E2C repressor limits productive replication of human papillomavirus. J Virol 88:937–947. https://doi.org/10.1128/JVI.02296-13.
68. Stubenrauch F, Zobel T, Iftner T. 2001. The E8 domain confers a novel long-distance transcriptional repression activity on the E8E2C protein of high-risk human papillomavirus type 31. J Virol 75:4139–4149. https://doi.org/10.1128/JVI.75.9.4139-4149.2001.
69. Stubenrauch F, Hummel M, Iftner T, Laimins LA. 2000. The E8E2C protein, a negative regulator of viral transcription and replication, is required for extrachromosomal maintenance of human papillomavirus type 31 in keratinocytes. J Virol 74:1178–1186. https://doi.org/10.1128/jvi.74.3.1178-1186.2000.
70. Zobel T, Iftner T, Stubenrauch F. 2003. The papillomavirus E8-E2C protein represses DNA replication from extrachromosomal origins. Mol Cell Biol 23:8352–8362. https://doi.org/10.1128/MCB.23.22.8352-8362.2003.
71. Chappell WH, Gautam D, Ok ST, Johnson BA, Anacker DC, Moody CA. 2015. Homologous recombination repair factors Rad51 and BRCA1 are necessary for productive replication of human papillomavirus 31. J Virol 90:2639–2652. https://doi.org/10.1128/JVI.02495-15.
72. Anacker DC, Gautam D, Gillespie KA, Chappell WH, Moody CA. 2014. Productive replication of human papillomavirus 31 requires DNA repair factor Nbs1. J Virol 88:8528–8544. https://doi.org/10.1128/JVI.00517-14.
73. Gillespie KA, Mehta KP, Laimins LA, Moody CA. 2012. Human papillomaviruses recruit cellular DNA repair and homologous recombination factors to viral replication centers. J Virol 86:9520–9526. https://doi.org/10.1128/JVI.00247-12.
74. Bristol ML, James CD, Wang X, Fontan CT, Morgan IM. 2020. Estrogen attenuates the growth of human papillomavirus-positive epithelial cells. mSphere 5:e00049-20. https://doi.org/10.1128/mSphere.00049-20.
75. James CD, Prabhakar AT, Otoa R, Evans MR, Wang X, Bristol ML, Zhang K, Li R, Morgan IM. 2019. SAMHD1 regulates human papillomavirus 16-induced cell proliferation and viral replication during differentiation of keratinocytes. mSphere 4:e00448-19. https://doi.org/10.1128/mSphere.00448-19.
76. Evans MR, James CD, Loughran O, Nulton TJ, Wang X, Bristol ML, Windle B, Morgan IM. 2017. An oral keratinocyte life cycle model identifies novel host genome regulation by human papillomavirus 16 relevant to HPV positive head and neck cancer. Oncotarget 8:81892–81909. https://doi.org/10.18632/oncotarget.18328.
77. Massimi P, Pim D, Bertoli C, Bouvard V, Banks L. 1999. Interaction between the HPV-16 E2 transcriptional activator and p53. Oncogene 18:7748–7754. https://doi.org/10.1038/sj.onc.1203208.
78. Końca K, Lankoff A, Banasik A, Lisowska H, Kuszewski T, Góźdź S, Koza Z, Wojcik A. 2003. A cross-platform public domain PC image-analysis program for the comet assay. Mutat Res 534:15–20. https://doi.org/10.1016/s1383-5718(02)00251-6.
79. James CD, Das D, Morgan EL, Otoa R, Macdonald A, Morgan IM. 2020. Werner syndrome protein (WRN) regulates cell proliferation and the human papillomavirus life cycle during epithelial differentiation. mSphere 5:e00858-20. https://doi.org/10.1128/mSphere.00858-20.